

2340

Intravoxel B0 Corrected Image Reconstruction with RF Prephasing

Steven T. Whitaker¹, Jon-Fredrik Nielsen², and Jeffrey A. Fessler¹¹Electrical Engineering and Computer Science, University of Michigan, Ann Arbor, MI, United States, ²Biomedical Engineering, University of Michigan, Ann Arbor, MI, United States

Synopsis

Regions with large intravoxel B0 gradients result in a wide spread of off-resonance frequencies within each voxel, causing spins within a voxel to dephase with respect to each other. Using model-based reconstruction to account for this dephasing can help alleviate artifacts from this signal loss, but success is limited in areas of extreme dephasing. We propose a model-based reconstruction method that includes RF prephasing to help mitigate the effects of extreme dephasing. We demonstrate that the proposed approach successfully recovers signal in areas of extreme dephasing and results in lower reconstruction error than model-based reconstruction without RF prephasing.

Introduction

Various MRI methods require acquiring signal with either a long readout and/or a long TE (e.g., fMRI, multi-gradient echo sequences, etc.), allowing a long time for off-resonance precession to occur. In areas of relatively constant B0 field inhomogeneity, this precession impacts only the phase of the image. However, in voxels having large B0 gradients, spins within a single voxel can dephase with respect to each other, inducing signal loss in the reconstructed image.

Using model-based reconstruction to account for this intravoxel dephasing can help alleviate artifacts from this signal loss¹⁻³. However, in areas of severe signal loss such as near the sinuses, such reconstruction can fail to fully recover the image. Therefore, in this work we propose to combine model-based reconstruction with the use of a *prephasing* RF pulse so that the intravoxel spread of spins is approximately zero at the echo time, mitigating the associated signal loss. We incorporate the effects of this prephasing into a model-based reconstruction method and demonstrate improved reconstructed images.

Theory and Methods

Regularized model-based reconstruction for multi-channel data involves solving

$$\operatorname{argmin}_{\mathbf{x}} \sum_{c=1}^C \frac{1}{2} \|\mathbf{A}_c \mathbf{x} - \mathbf{y}_c\|_2^2 + \lambda R(\mathbf{x}), \quad (1)$$

where \mathbf{x} is the image to recover, \mathbf{y}_c is the k-space data from coil c , \mathbf{A}_c is the system model mapping from image space to k-space for coil c , C is the total number of coils, R is a regularizer, and λ is a tuning parameter. To account for intravoxel B0 effects and RF prephasing, \mathbf{A}_c is given by

$$\mathbf{A}_c = (\mathbf{W} \odot \mathbf{F}) \Phi \mathbf{S}_c \mathbf{x}, \quad (2)$$

where \mathbf{S}_c is a diagonal matrix of coil sensitivity, Φ is a diagonal matrix containing the bulk phase imparted to each voxel by the prephasing pulse, \mathbf{F} is the Fourier operator, and \odot is elementwise product. \mathbf{W} is a matrix describing intravoxel dephasing effects with entries^{3,4}

$$W_{mm} = e^{-i2\pi f_n t_m} \operatorname{sinc}_3((\mathbf{k}_m + \mathbf{g}_n t_m + \gamma_n) \odot \Delta), \quad (3)$$

where n indexes spatial location, m indexes k-space sample time, f_n is the off-resonance frequency, t_m is the k-space sample time, sinc_3 is the 3D sinc function, \mathbf{k}_m is the k-space location, \mathbf{g}_n is the spatial gradient of the B0 field map, γ_n is the spatial gradient of the RF prephasing phase map, and Δ is the voxel size. Note that Φ and γ_n are the key new aspects that incorporate the effects of RF prephasing into the proposed model-based reconstruction method. An ideal RF prephasing pulse will impart phase such that $f_n \text{TE} + \phi_n = 0$ (where ϕ_n is the n th diagonal entry of Φ) and an intravoxel spread of phase such that $\mathbf{g}_n \text{TE} + \gamma_n = \mathbf{0} \quad \forall n$; i.e., all spins throughout the object will be in phase at the echo time.

In this work, we compare model-based image reconstructions modeling intravoxel B0 effects with and without RF prephasing. We used the ℓ_2 -norm of 3D finite differences for the regularizer with $\lambda = 0.1$. We approximated \mathbf{W} using a low-rank approximation³.

For the simulation experiments, we used a digital BrainWeb phantom⁵ and four synthetic coil sensitivity maps. We generated an off-resonance map with values 0–85 Hz and a spatial gradient with values -60–7.3 Hz/voxel (see Figure 1). We simulated a $64 \times 64 \times 3$ matrix size Cartesian stack-of-EPI readout occurring from 3 to 40 ms with TE = 21.6 ms for each z phase encode. In one experiment, RF prephasing was specified such that all spins were in phase at the echo time. In another experiment, we varied the RF prephasing to rephase the spins at different times to investigate how RF prephasing accuracy can benefit reconstructed image quality.

Results

Figure 2 shows a reconstruction that does not account for intravoxel B0 effects. The overlaid contours draw a connection between the resultant signal loss and the corresponding value of the 3D sinc term in (3).

Figure 3 compares a reconstruction that does not account for intravoxel B0 effects to one that does, but without RF prephasing, and to one that includes both intravoxel B0 effects and RF prephasing. Each incremental addition to the model improves the reconstructed image, as verified by the normalized root mean square error (NRMSE) values reported in Table 1(a). Figure 3 also demonstrates that RF prephasing alone (without modeling intravoxel effects)

is not enough to recover the true image, emphasizing the importance of the proposed reconstruction method.

Figure 4 demonstrates what happens when the RF prephasing refocuses spins at different times. As expected, the closer to TE, the better, but there is still marked improvement even with refocusing occurring well before the echo time (e.g., when refocusing at 10 ms), as verified by the NRMSE values in Table 1(b).

Discussion and Conclusion

We introduced incorporating RF prephasing into model-based reconstruction including intravoxel B0 effects. The resultant reconstruction is better visually and in terms of NRMSE than when RF prephasing is not used in simulation.

Future areas of research include validating these simulation results with in vivo results, developing algorithms for designing RF prephasing pulses based on spectral⁶ and/or spatial^{7,8} excitation profiles, and using the proposed method in an fMRI study to see how the fMRI activation maps are impacted.

Acknowledgements

This work was supported in part by NIH grants R21 AG061839 and U24 NS120056 and by NSF grant IIS 1838179.

References

- [1] B. P. Sutton, D. C. Noll, and J. A. Fessler. Compensating for within-voxel susceptibility gradients in BOLD fMRI. In Proc. Intl. Soc. Mag. Res. Med., page 349, 2004.
- [2] Y. Zhuo and B. P. Sutton. Iterative image reconstruction model including susceptibility gradients combined with Z-shimming gradients in fMRI. In embc, pages 5721–4, 2009.
- [3] F. Lam and B. P. Sutton. Intravoxel B0 inhomogeneity corrected reconstruction using a low-rank encoding operator. Mag. Res. Med., 84(2):885–94, August 2020.
- [4] J. A. Fessler and D. C. Noll. Model-based MR image reconstruction with compensation for through-plane field inhomogeneity. In Proc. IEEE Intl. Symp. Biomed. Imag., pages 920–3, 2007. Invited paper.
- [5] D. L. Collins, A. P. Zijdenbos, V. Kollokian, J. G. Sled, N. J. Kabani, C. J. Holmes, and A. C. Evans. Design and construction of a realistic digital brain phantom. IEEE Trans. Med. Imag., 17(3):463–8, June 1998.
- [6] J. Asslander, S. J. Glaser, and Juergen Hennig. Spin echoes in the regime of weak dephasing. Mag. Res. Med., 75(1):150–60, January 2016.
- [7] T. Luo, D. C. Noll, J. A. Fessler, and J-F. Nielsen. Joint design of RF and gradient waveforms via auto-differentiation for 3D tailored excitation in MRI. IEEE Trans. Med. Imag., 2021.
- [8] C. Yip, D. Yoon, V. Olafsson, S. Lee, W. A. Grissom, J. A. Fessler, and D. C. Noll. Spectral-spatial pulse design for through-plane phase precompensatory slice selection in T2*-weighted functional MRI. Mag. Res. Med., 61(5):1137–47, May 2009.

Figures

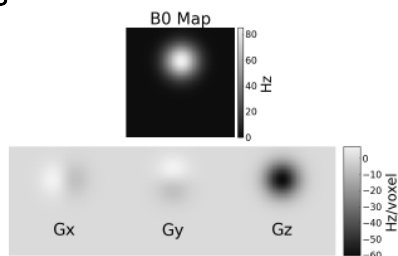


Figure 1: B0 field map and its spatial gradients in each direction used in simulation. The B0 gradients in the x and y directions range from -7.3 to 7.3 Hz/voxel. For TE = 21.6 ms, this corresponds to 1/6 cycle/voxel. In the z-direction, the peak of 60 Hz is more than one cycle/voxel.

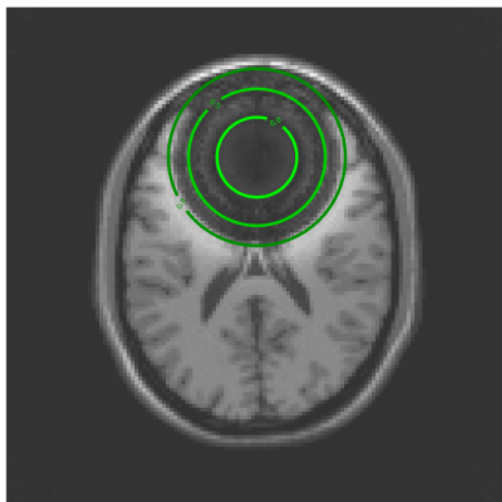


Figure 2: Illustration of the connection between the value of the 3D sinc in equation (3) and the corresponding signal loss seen in an image reconstructed without correcting for the effect. The three contour lines shown correspond to values 0, 0.5, and 0.8.

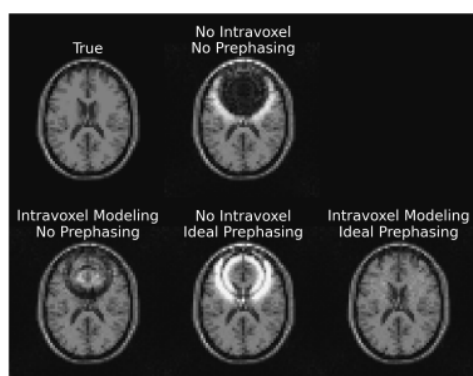


Figure 3: Comparison of images reconstructed without modeling intravoxel B0 effects (with and without ideal RF prephasing), with such modeling but without RF prephasing, and with ideal RF prephasing and modeling both intravoxel B0 effects and RF prephasing with the proposed model-based image reconstruction method. RF prephasing results in significantly improved recovery of the true underlying image when it is combined with modeling intravoxel dephasing.

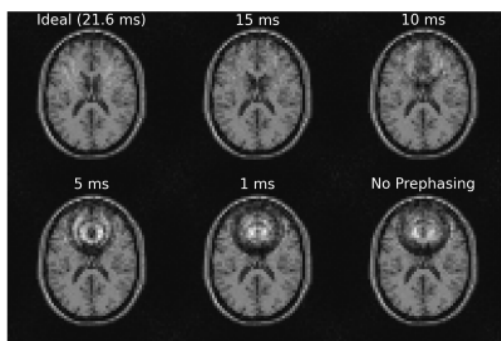


Figure 4: Comparison of different amounts of RF prephasing when combined with the proposed model-based image reconstruction method that accounts for both intravoxel dephasing and the effects of partial RF prephasing. Increasing the time at which the spins rephase from 0 ms (no prephasing) to 21.6 ms (TE, the ideal case) improves the reconstruction quality. Even at 10 ms there is significant improvement over no prephasing.

(a)

	NRMSE
No modeling of intravoxel dephasing, no RF prephasing	32.0%
No modeling of intravoxel dephasing, ideal RF prephasing	38.8%
Modeling of intravoxel dephasing, no RF prephasing	7.5%
Modeling of intravoxel dephasing, ideal RF prephasing	1.0%

(b)

Rephasing Time	NRMSE
0 ms	7.9%
1 ms	8.5%
5 ms	7.3%
10 ms	3.3%
15 ms	1.4%
21.6 ms (TE)	1.2%

Table 1: (a) NRMSE values for reconstructed images shown in Figure 3. (b) NRMSE values for reconstructed images shown in Figure 4. In both cases, the proposed combination of RF prephasing and model-based reconstruction led to the best image quality.